Title

Probing Self-Assembly in Arginine—Oleic Acid Solutions with Terahertz Spectroscopy and X-ray Scattering

Journal

The Journal of Physical Chemistry Letters, 11(21)

ISSN

1948-7185

Authors

Lu, Wenchao

Zhang, Emily

Amarasinghe, Chandika

et al.

Publication Date

2020-11-05

DOI

10.1021/acs.jpclett.0c02593

Peer reviewed

Probing self-assembly in arginine-oleic acid solutions with terahertz spectroscopy and X-ray scattering

Wenchao Lu,[a] Emily Zhang,[a,b] Chandika Amarasinghe,[a] Oleg Kostko [a] and Musahid Ahmed [a*]

[a] *Chemical Sciences Division, Lawrence Berkeley National Laboratory, Berkeley, California 94720,* USA

[b]*College of Chemistry, University of California, Berkeley, California 94720, USA*

[*] *E-mail: mahmed@lbl.gov*

Abstract

A study of the formation of microstructures in the reaction of oleic acid with arginine elucidates dynamical self-assembly processes at the molecular level. Terahertz spectroscopy combined with density functional calculations reveals the initial hydrogen bonding motifs in the assembly process, leading to the formation of micelles and vesicles. Small-angle X-ray scattering measurements allow for kinetic analysis of the growth processes of these nanostructures, revealing a pre-nucleation pathway of vesicles and micelles which lead to sponge-like structures. This final stage of the assembly into sponge-like aggregates is investigated with optical microscopy. The formed structures only occur at pH > 8 and are resistant to extreme acidic and basic conditions. A mechanistic pathway to the formation of the sponge-like aggregates is described.

TOC graphic:

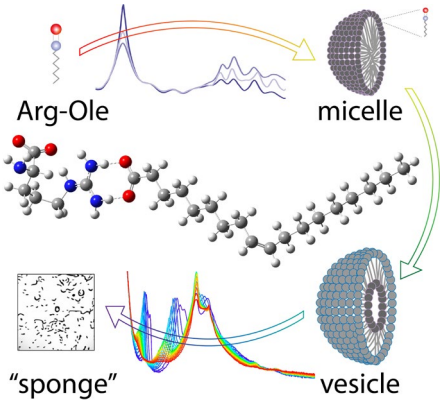

Nucleation and subsequent crystallization/aggregation is at the heart of various scientific disciplines, however, the understanding of the molecular mechanisms underlying phase separation and the formation of the first solid particles in aqueous solution is rather limited.[1] The role of pre-nucleation clusters as solute precursors in the emergence of a new phase is a theme that is being pursued to understand crystallization and aggregation beyond classical nucleation theory.[2] This has enormous ramifications for the self-assembly of natural or synthetic amphiphiles to build well-defined nanostructures with controllable function at the molecular level, which are driven by non-covalent interactions. We seek to develop the link between the chemical speciation of homogeneous solutions and the process of phase separation using arginine as a test case of biomolecule assembly followed by its reaction with oleic acid to form self-assembled nanostructures. Arginine has a flexible molecular structure, composed of a guanidinium head group and α-amino acid tail held together by an aliphatic hydrocarbon backbone. The protonation of the guanidinium group and the deprotonation of the carboxyl group leads to a zwitterionic structure. Coupled with the unique properties of the planar guanidinium group, this allows for intermolecular and intramolecular interactions, such as hydrogen bonding and ionic interactions, which leads to very interesting solvation, nucleation, and aggregation dynamics. This alteration in the strength of hydrophobic interactions allows for a strategy to tune it to optimize molecular recognition and self-assembly processes,[3] act as a glue for modulation of biomolecular function,[4] and find application in methods for cell penetration[5] and drug delivery.[6] It has been suggested that the guanidinium group in arginine can self-associate and act as a glue in protein and other biological assembly processes via stacking of the side chains in arginine residues and by salt bridges formed between the like-charge ion pair and the C-terminal carboxyl groups demonstrated recently using SAXS and theoretical calculations.[7] Early work using electrospray mass spectrometry also alluded to cluster formation in arginine solutions (albeit in very low concentrations at 10^{-4} M and pH = 3.1)[8] while large clusters are also implicated in liquid fatty acids, which are saturated and can aid in nucleation and subsequent crystallization.[9]

Zhang and co-workers,[6b, 6c, 10] in a series of papers, studied the phase behavior and self-assembling properties of unsaturated fatty acids with arginine as a function of external conditions (pH and temperature).

In the case of oleic acid, using microscopy, transmission electron microscopy (TEM), and IR analysis of titration curves, they postulated a tentative molecular mechanism for the rich structural dynamics displayed in the system. They put down the observed formation of micelles, vesicles, and sponges under various conditions due to the subtle interplay of electrostatic-hydrophobic interactions and hydrogen bonding. In another study, a low-level molecular dynamics calculation[11] of the free energy landscape in arginine oleic acid interactions showed the guanidinium groups encounter an energy barrier 3 times weaker to bind fatty acids relative to amino groups. However, a clear molecular-level picture of kinetics and mechanistic details remain elusive, notwithstanding these studies, and we devised an experimental approach to use molecular and structural tools to probe the structural growth processes in the aqueous arginine-oleic acid (Arg-Ole) system.

We used terahertz (THz) time-domain spectroscopy and small-angle X-ray scattering (SAXS) to probe the growth kinetics and density functional theory (DFT) calculations to corroborate the structural and spectroscopic details obtained in the experiment. THz radiation provides a means to probe phase changes and hydrogen bond dynamics in aqueous solutions. For instance, phase changes that lead to subsequent crystallization from aqueous solutions have been revealed by probing the water dynamics in aqueous $CaCO_3$[12] and tartaric acid solutions[13] with THz spectroscopy. Recently, THz time-domain spectroscopy has been used to probe the ion-induced changes in water dynamics and lipid structure in vesicles[14] and micelles[15]. X-ray scattering has proven to be an invaluable tool in probing structure in both ordered and disordered media, particularly in the 1 – 100 nm size regime with SAXS, and is finding increased use for *in-situ* probing of nucleation and crystallization processes in aqueous media. In the context of understanding pre-nucleation complexes in growth mechanisms, glycine (the smallest amino acid) has been studied with dynamic light scattering[16] and also SAXS.[17] Very recently, the self-assembly in glycolipids (glucose-disaccharides with an oleic acid tail) as a function of pH was used to track the formation of micelles, fibers, vesicles, and bilayers. The importance of deprotonation of the carboxyl group in the acid tail was highlighted via simulated fits to the SAXS pattern.[18] Another recent *in-situ* SAXS study of polymerization

induced self-assembly in aqueous emulsions provides a framework and model to extract structural information, particularly nucleation and micelle formation from an analysis of the scattering patterns.[19]

The experiments to measure growth was performed in a quartz cuvette in the case of THz radiation and in a quartz capillary for the SAXS measurements and are described in the experimental section. Oleic acid was added to arginine solution at different concentrations in a quartz cuvette (THz) or capillary (SAXS), resulted in the formation of white aggregates instantly and steadily grew at the interface of the two liquid phases (inset of **Fig 1c**). **Fig. 1** shows the experimental results for the first 10 minutes of reaction time under each condition, with t_0 being set to when the reaction began. Spectra were collected at different pH values ranging from 2 to 11. To investigate concentration effects, we choose 0.7, 0.5 and 0.1M of arginine solution at pH = 11. The THz spectra (**Fig. 1b – 1d**) reveals four absorption bands: 0.3, 1.2, 1.5 and 2.4 THz. The peak at 1.5 THz only becomes significant at higher concentrations (0.5 M and 0.7 M), and its intensity increasing with time, possibly arising from the formation of the aggregates at the liquid interface. The intensity profiles increase more rapidly with time and concentration, notice how the 0.7M concentration shows much more apparent changes within 10 min compared to the case of 0.1M.

Previous studies have suggested that, in aqueous solution, arginine shows a monotonically increasing absorption spectrum which broadly resembles the spectrum of pure water (**Fig. S1** in **SI**);[20] in contrast, in a microcrystalline form (several tens of microns), it shows a peak at around 1.0 THz at room temperature, which becomes very sharp with a decrease in temperature and shifts to the blue.[21] This was attributed to arise from anharmonic intermolecular vibrational modes in the microcrystal. THz spectroscopy has also been used to probe oleic acid and oleic acid-water mixtures (together with rapeseed oil).[22] Crystalline forms of saturated fatty acids (even numbers of carbon, between 12 – 20) were measured with THz spectroscopy between 0.5 to 3 THz between 96 and 293 K.[23] Three frequency bands were identified at low temperature which progressively disappeared with an increase in temperature. DFT calculations suggested that these peaks arose from large amplitude motion of the carbon tails about the central carboxylate head. From the literature data and comparing to our own measurements, we deduce that the spectrum at the interface of arginine and oleic acid cannot occur from either aqueous arginine or oleic acid.

To understand the THz spectral contribution of the white aggregate at the interface, DFT calculations were carried out with a polarizable continuum model (PCM) which can account for dispersion forces of bulk water. Previously we had used this model to develop pH-dependent structures in arginine to explain experimental observations in the photoelectron spectrum and mass spectrometry in aqueous aerosols.[24] On the basis of our previous study,[24] four arginine tautomers (*z*-, *zat*-, *t*-, and *c*-) were extracted to build Arg-Ole monomer in the current study. Several Arg-Ole conformers built upon *z*- and *zat*-Arg tautomers were obtained and remain at lower relative Gibbs free energy at 298K (ΔG), whereas those built upon *c*- and *t*-Arg have ΔG at least 15 kcal/mol higher. **Fig. 1a** presents the most stable conformer for each tautomer category. All the other geometries of Arg-Ole conformers considered in the current study together with their THz spectra are summarized in **Fig. S2 – S3** in **SI**. The DFT results revealed that for each conformer, the arginine moiety is paired with oleic acid via two hydrogen bonds between the guanidinium group of arginine and carboxyl group of oleic acid. We also discovered that certain optimizations converged to non-hydrogen bonded pairs, with lower electronic energies but at much higher ΔG. In the context of free energies and self-assembly, Whitelam et al. has reviewed several self-assembly pathways and ascribed them into two categories:[25] the first category starts from a near-equilibrium assembly state and has a relatively simple free-energy surface. The process could be a single step or multiple steps, with $\Delta G < 0$ for each step. The second category is far from equilibrium, and the free-energy surface is biased by dynamic effects. The Arg-Ole system, which follows a multiple-step liquid-to-aggregate pathway triggered by isotropic short-range interactions, falls within the first category, and the overall free energy reduces as the self-assembly proceeds. As a result, these non-hydrogen bonded Arg-Ole structures can be safely ignored because high ΔG prevents the self-assembly processes and cannot be captured within the timescales of our measurement.

The THz spectra for the most stable conformers of *z*- and *zat*- tautomers are calculated and shown in red and green lines labeled as 1 and 2 in **Fig. 1b**, and the peak positions are associated with the vibrational modes of hydrogen bonds between arginine and oleic acid (**Fig. S4 – S5** in **SI**). A superimposition of the two conformers weighed by their population at 298K is shown as a thick black curve in **Fig. 1b – 1d**, and assists in describing the THz profile. We tentatively suggest that the THz peaks correlating to the calculated

single Arg-Ole monomer provide a qualitative picture of the hydrogen bonding network measured within the white aggregate and is not an artifact of the measurement. The Arg-Ole aggregates exhibit a much larger molecular flexibility due to the nature of a sponge-like structure without a repetitive crystal lattice. Similarly, the THz calculation based on Arg-Ole monomer within a solvation cavity suggests a relatively larger amplitude of motions compared to crystals, which is in agreement with our experimental observations.

Fig. 1e – 1g present the SAXS spectra recorded for 0.7, 0.5, and 0.1M of arginine with oleic acid, with concentrations and reaction conditions being the same as previously used for THz spectroscopy. From the SAXS spectra, we can extract the average sizes of the particles from the Q-vector (x-axis) and the intensity is represented in the y-axis. The intensity within each measured dataset is poorly reproducible since the X-ray beam might not probe the same density of particles, and there could be diffusion between the interfacial aggregation region and neighboring liquid phases. However, the Q-vector remains highly reproducible for each dataset, indicating a reliable averaged particle size formed inside the liquid mixture, and thus shows a statistical significance (see **Fig. S6 – S8** in **SI** for all the SAXS datasets). The SAXS spectral evolutions of time for the three concentrations are summarized in **Fig. 1e – 1g**. The four peak positions at 0.13, 0.11, 0.08, and 0.03Å^{-1} correlate to averaged particle sizes of 48, 55, 80, and 180Å respectively. A composite peak around 0.12Å^{-1} is present regardless of concentration, with the peak intensities growing stronger as the concentration increases, particularly correlating to higher particle number densities. It should be noted that the peaks from SAXS spectra are composite, and the positions of the peaks at 0.08 and 0.03Å^{-1} drift along with time. Thus, the calculated particle sizes shown above are a qualitative descriptor of the average size. Previous studies proposed that the entire self-assembly process may experience multiple phases, depending on the concentration of reactants, and that micro-structures of different sizes coexist within the liquid mixture.[6a, 6b] Starting from individual Arg-Ole monomers, they first aggregate into micelles, and then grow up to vesicles or multilayered structures, and finally to large-scale sponge-like aggregates.[6a, 6b] Our DFT calculation shows that for each stable Arg-Ole monomer, the approximate head-to-tail length is around 20Å. Thus, we deduce that the wide composite peak of 50Å should correspond to micelle- and vesicle-type

structures, while the 80 and 180Å peaks correspond to larger multilayered structures and can act as seeds for building into sponge-like aggregates.

Amino acids tend to protonate and deprotonate as a function of pH, and this has profound implications in self-assembly processes and can provide a mechanistic handle to the processes occurring here. The absence of a detectable interface (white aggregates) between the two liquid phases below pH = 8 suggests that self-assembly is absent under near neutral and acidic conditions (inset of **Fig. 2b**). This is confirmed in the THz and SAXS spectra, where no changes are observed for up to an hour, as seen in **Fig. 2b – 2c**. While some ripples might be observed in the THz spectrum, it did not show any strong correlation with the DFT calculated spectra, in stark contrast to basic conditions shown in **Fig. 1b – 1d**. Previous studies also reported that the reaction rate of the Arg-Ole system only became significant above pH = 9.[6] It has been suggested that the self-assembly process between arginine and a long-chain carboxylic acid is controlled by the pK_a of the carboxylic acid, on the basis that the carboxyl group is responsive to pH change, switching between -COOH and -COO^- via deprotonation, and only the deprotonated -COO^- is capable in forming two stable hydrogen bonds with the guanidinium group of arginine.[6b, 26] Oleic acid has a pK_a of 9.85[27] and a calculation of the fractional composition (**Fig. S9** in **SI**) confirms that an appreciable population of oleate anion begins to emerge only when pH > 8. Similarly, arginine has multiple ionization states (Arg, $ArgH^+$, $Arg2H^{2+}$ and $[Arg–H]^-$), and all the neutral and positive ionization states are capable of forming hydrogen bonds except for $[Arg–H]^-$ (only dominant at pH = 14) due to intermolecular Coulombic repulsion. Thus, the pH dependence of self-assembly in the arginine and oleic acid can be explained by this molecular mechanism.

A factor to consider in self-assembly is the process of reversibility, indeed, unsaturated fatty acids can easily self-assemble into micelles and vesicles and these structures are reversible by adjusting the pH value.[28] In comparison, micelles, and vesicles formed in the Arg-Ole system serve as transition structures that contribute to the formation of macroscopic sponge-like aggregates as seen in the SAXS analysis. It remains questionable whether the formation of these sponge-like aggregates is reversible by varying the pH value. With this in mind, we first added strong acid and base to the white aggregate to tune the pH from 0

to 14 (**Fig. S10** in **SI**). However, the white aggregate remained stable and did not dissolve back into the liquid phase. The only change is that the liquid phase was emulsified at neutral and acidic pH since the addition of acid neutralized the oleate anion and broke down the micelles and vesicles formed by the oleate anions themselves. Another trial started from mixing arginine solution of pH = 7 with oleic acid with no reactions observed. By slowly and carefully adding the base solution, white aggregates formed and remained resistant to the variation of pH value. Such observation confirms that the final-stage sponge-like structure is thermodynamically very stable and provides us an impetus to look more into its structure and morphology.

Previous TEM studies in the Arg-Ole system suggest a complex multiphase dynamical environment with changes in concentration and pH.[6] With an increase in arginine concentration, micelles formed, followed by a coexisting binary system consisting of micelles and vesicles, then a ternary system which included sponge-like structures and a final binary phase of sponges and oil phase. These experiments were performed at fairly low concentrations and all the samples were equilibrated until a steady state was reached, in contrast to our high concentration and pH approach to probe instantaneous dynamics of self-assembly where the system is far from equilibrium. Whereas earlier, we attempted with THz and SAXS spectroscopy to extract a structural picture at the molecular level of the dynamic events, we now perform optical microscopy to examine the phase system at longer timescales to obtain information on the emerging sponge-like structures. The most interesting aspects of the dynamics revealed from THz and SAXS occur at the interface of the two liquid phases and we now focus on that part. Optical microscopy reveals that as the two liquid phases came into contact, they merged into a larger liquid bulge a few millimeters in size, within which tiny aggregate cores began to grow and coagulate into larger ones driven by surface tension and diffusion. Within minutes, the aggregates grew to the millimeter scale and sponge-like structures were observed (**Fig. 3a**). A cross section of the aggregates was extracted by cleaving it with a cover slide (1 × 1" in size) and the subsequent image reveals the framework of the sponge-like aggregates surrounded by numerous tiny liquid droplets (**Fig. 3b**).

The SAXS spectral profiles in **Fig. 1** show changes within the first 10 min, which allow for kinetic analysis for the Arg-Ole systems at different concentrations and pH = 11. As pointed out previously, the SAXS intensity is poorly reproducible due to the sensitivity of the position where the X-ray beam hits, and the non-uniformity of the particle density caused by diffusion. However, the particle size (calculated from Q-vector) of each dataset has good reproducibility and thus is suitable for kinetic analysis (see **Fig. S11 – S13** in **SI** for all the datasets). For 0.1M arginine with oleic acid, we only see the composite peak related to 50Å, and its size remains unchanged along the time axis (**Fig. 4a**). This correlates to the initial stages of assembly from the Arg-Ole pair to micelles and vesicles, which is in dynamic equilibrium. The density of the particles (reflected by the SAXS intensity) slowly accumulates over time; however, the low concentration does not boost the buildup into larger multilayered structures. As the concentration increases, for 0.5M and 0.7M arginine, another two groups of peaks begin to emerge besides the 50Å composite peak, relating to an average size of 80 and 180Å (**Fig. 4b – 4c**). As seen in **Fig. 1e – 1g**, the particle density at the interface steadily increases. The stabilization of the intensity for 0.7M arginine indicates saturation of micelles/vesicles around 5 min, accompanied by the consumption of these smaller structures for the formation of larger seed aggregates. Immediately after the reaction begins, another two peaks emerged, corresponding to the larger multilayered structures that are gradually aggregating from smaller micelles/vesicles. It is interesting that the sizes of those larger multilayered structures, unlike micelles and vesicles, increases with time, suggesting that the micelle/vesicles are acting as pre-nucleating complexes and are metastable in nature. Mechanistically, these multilayered structures serving as building blocks are necessary for the construction of large-scale sponge-like aggregates visible under optical microscopy. From **Fig. 4b** and **4c**, the slopes of the lines corresponding to multilayered structures indicate the "buildup rate". For 0.5M arginine with pure oleic acid, the "buildup rate" of multilayered structures is slower compared to that of 0.7 M Arg-Ole. The rate constant for growth at 0.7 M Arg-Ole is evaluated as 3 – 10 Å/min. This confirms that the buildup process is concentration-dependent, and a higher concentration boosts the formation of larger-scale structures.

We herein propose the initial stage mechanism for the self-assembly process of Arg-Ole, focusing on the first 10 min immediately after the reaction occurs, when the conditions within the reactants are far from reaching a steady state and controlled via diffusion. Thus, multiple phases of self-assembly adducts may coexist simultaneously. Right after the instant that two liquid phases mingle with each other, arginine and oleic acid dispersed within the solution are immediately paired via hydrogen bonds and aggregate into micelles. Then, more Arg-Ole pairs adhere to and assemble into vesicles for the reduction of the total free energy and equilibrate. The successive buildup process into seed aggregates is observed by SAXS spectra, and aggregate size up to 200Å is captured. This process is also dependent on the concentration of reactants, as a higher concentration can accelerate the buildup process. These seed aggregates work as the building block for the construction into larger-scale sponge-like structures held together by the hydrogen-bonding network of water. At the final equilibration state, white aggregates emerge at the interface of liquid phases which is visible with optical microscopy. Microscopically, a molecular understanding of such sponge-like aggregates also emerges from an analysis of the THz spectra and correlated to DFT calculations.

To conclude, this study provides a dynamic and kinetic perspective on the growth mechanisms at a molecular level for Arg-Ole, which expands on previous phase transition mechanisms and the corresponding morphology at the steady state. The existence of a non-classical pathway to growth will provide impetus to new experimental and theoretical investigations to probe this system. The stability of the sponge-like aggregates under strong acidic and basic conditions could potentially pave the way for developing biocompatible functional materials.

Experimental Section

Chemicals. Oleic acid was purchased from Sigma Aldrich (analytical grade) and L-arginine from Fluka (99%, NT). Three arginine solutions with concentrations of 0.1, 0.5, and 0.7 M were prepared using deionized water followed by adding pure oleic acid. Hydrochloric acid (37%, Sigma Aldrich) and sodium hydroxide solution (2M, Titripur) were diluted and used to adjust the pH of the arginine samples in the range of 0 to 14, measured by an Oaklon Instruments pH 510 Benchtop Meter.

Terahertz Spectroscopy. Terahertz (THz) spectra were recorded on a Menlo Systems TERA K15 spectrometer. Spectra of Time (ps) *vs.* Amplitude (mV) and Frequency (THz) *vs*. Intensity (dB) was obtained using the Menlo Systems Scan Control with the THz beam size of 3 mm (H) × 10 mm (W). The sample was placed in a quartz cell, with the dimension of 1 mm for both the window thickness and the sample thickness confined between the windows. The arginine solution of various concentrations was first added to the cell, and oleic acid was then added at the instant the spectrum collection began. The collection time for each spectrum was set to 100 seconds. Reference spectrum was scanned by placing an empty sample cell. The spectral resolution for the measurement based on a gas-phase line at 1.413 THz was 8 GHz. The environment was purged using nitrogen gas to reduce the effects of gas-phase air and water vapor. LabVIEW was used to automate data collection. THz spectra were analyzed using Menlo Systems TeraMAT software. The time-domain waveform was truncated to remove Fabry-Perot reflections in our measurements which reduced the high-frequency noise. A Newport Agilis Piezo Motor was installed to move the sample cell in the vertical direction perpendicular to the laser propagation with a step size of 1 mm. Datasets were collected by both scanning across the cuvette and by keeping the cuvette immobile at the interface position.

Small-Angle X-Ray Scattering. Small-angle X-ray Scattering (SAXS) measurements were conducted using 10 keV monochromatic X-rays at Beamline 7.3.3 of the Advanced Light Source, Lawrence Berkeley National Laboratory. The SAXS beam size is about ~ 300 μm (H) × 700 μm (W). During SAXS measurements, a thin-walled quartz capillary (1.5 mm O.D., Charles Supper Company) infused with arginine solution of various concentrations was placed horizontally in front of the X-ray beam shutter. Pure oleic acid was injected via a syringe pump immediately before SAXS measurements. The exposure time was set to 10s for each measurement, which was collected consecutively up to 10 min. A camera was placed near the capillary to monitor the instrumental conditions during measurements and provided snapshots at different times of reaction. Before the reaction, the distance from the capillary to the detector was calibrated using a silver behenate standard. The raw data were processed using the Nika package[29] embedded to Igor Pro 6.37 software to get the SAXS spectra of Q-vector to intensity.

Microscopy. The microscopic images were taken using a Zeiss (AXIO Examiner Z1) microscope with the magnification of 20 to 50 X. A mercury lamp was used and tuned for the illumination, and a computer-controlled CCD camera is connected to the ocular lens so that images could be taken directly from the computer program. During operation, a drop of each reactant was placed on a slide, and the eyesight was focused on the interface of the two liquid

phases. A cover slide was then used to sandwich the white Arg-Ole aggregates formed into a thin layer for clearer observation of the morphology.

Computational. All the calculations were performed using the Gaussian 09 package.[30] Geometries of arginine were optimized at ωB97XD/6-31g(d,p) level of theory with the polarizable continuum model (PCM)[31] for the implicit solvent effect and calculated structures together with its energetics were consistent with the literature.[24] Based on these geometries, the structures of Arg-Ole adducts at various ionization states are thus generated and optimized. Successively, frequency analyses were performed for each structure, and the corresponding spectra are convoluted to an FWHM of 0.1 THz for each THz spectrum. Zero-point energies and Gibbs free energy corrections were scaled by a factor of 0.974.[32] The convergence criteria we used for our calculation are the default ones with RMS force criterion to 3×10^{-4}. For those geometries that are difficult to converge, GDIIS method and ultrafine integration grid are used. It is well-known that the calculation of THz spectrum is notoriously difficult especially for solid crystalline states using single-molecule representation, which is due to a lack of accurate treatment of weak intermolecular interactions, especially the long-range forces.[33] However, in our case, the self-assembly aggregates exhibit a very loosely bounded structure being less similar to a repetitive crystal lattice in real crystals where strong intermolecular interactions exist. Such intrinsic structural difference of the Arg-Ole aggregates invalidates the solid-state calculation. On the other hand, the calculated THz spectrum for our system using single-molecule representation correlates quite well to the experiments and assures us the validity of our calculation.

Supporting Information

The THz spectra of Arg solutions, DI water and pure oleic acid; All Arg-Ole conformers considered in this study together with their calculated THz spectra; the most significant vibrational modes of *z*- and *zat*- conformer in Fig. 1a; all other SAXS datasets; the fractional composition charts of each ionization state for Arg and oleic acid; photos showing the stability of Arg-Ole aggregates at the pH range of 0 – 14; and kinetics of all datasets for comparison.

Acknowledgments

This work is supported by the Director, Office of Science, Office of Basic Energy Sciences, of the U.S. DOE under Contract No. DE-AC02-05CH11231, through the Condensed Phase, Interfaces, and Molecular Sciences Program. This research used resources of the Advanced Light Source, a Department of Energy (DOE) Office of Science User

Facility under the same contract. The authors thank D. J. Rosenberg, C. Zhu, and E. Schaible at the SAXS/WAXS beamline of the ALS for assistance with setting up experiments and data analysis.

References

1. Gebauer, D.; Raiteri, P.; Gale, J. D.; Cölfen, H., On classical and non-classical views on nucleation. *Am. J. Sci.* **2018,** *318* (9), 969-988.
2. Gebauer, D.; Kellermeier, M.; Gale, J. D.; Bergström, L.; Cölfen, H., Pre-nucleation clusters as solute precursors in crystallisation. *Chem. Soc. Rev.* **2014,** *43* (7), 2348-2371.
3. Ma, C. D.; Wang, C.; Acevedo-Vélez, C.; Gellman, S. H.; Abbott, N. L., Modulation of hydrophobic interactions by proximally immobilized ions. *Nature* **2015,** *517* (7534), 347-350.
4. Mogaki, R.; Hashim, P. K.; Okuro, K.; Aida, T., Guanidinium-based "molecular glues" for modulation of biomolecular functions. *Chem. Soc. Rev.* **2017,** *46* (21), 6480-6491.
5. Herce, H. D.; Garcia, A. E.; Cardoso, M. C., Fundamental molecular mechanism for the cellular uptake of guanidinium-rich molecules. *J. Am. Chem. Soc.* **2014,** *136* (50), 17459-17467.
6. (a) Li, G.; Yang, Q.; Song, A.; Hao, J., Self-assembled structural transition from vesicle phase to sponge phase and emulsifying properties in mixtures of arginine and fatty acids. *Colloids Surf. A Physicochem. Eng. Asp.* **2015,** *487*, 198-206; (b) Wang, Y.; Jiang, L.; Shen, Q.; Shen, J.; Han, Y.; Zhang, H., Investigation on the self-assembled behaviors of C18 unsaturated fatty acids in arginine aqueous solution. *RSC Adv.* **2017,** *7* (66), 41561-41572; (c) Wang, Y.; Jiang, L.; Wei, C.; Zhang, H., Phase behaviors and self-assembled properties of ion-pairing amphiphile molecules formed by medium-chain fatty acids and l-arginine triggered by external conditions. *New J. Chem.* **2017,** *41* (23), 14486-14497.
7. (a) Tesei, G.; Vazdar, M.; Jensen, M. R.; Cragnell, C.; Mason, P. E.; Heyda, J.; Skepö, M.; Jungwirth, P.; Lund, M., Self-association of a highly charged arginine-rich cell-penetrating peptide. *PNAS* **2017,** *114* (43), 11428-11433; (b) Vazdar, M.; Heyda, J.; Mason, P. E.; Tesei, G.; Allolio, C.; Lund, M.; Jungwirth, P., Arginine "magic": guanidinium like-charge ion pairing from aqueous salts to cell penetrating peptides. *Acc. Chem. Res.* **2018,** *51* (6), 1455-1464.
8. Kellermeier, M.; Rosenberg, R.; Moise, A.; Anders, U.; Przybylski, M.; Cölfen, H., Amino acids form prenucleation clusters: ESI-MS as a fast detection method in comparison to analytical ultracentrifugation. *Faraday Discuss.* **2012,** *159* (0), 23-45.
9. Noël, J. A.; LeBlanc, L. M.; Patterson, D. S.; Kreplak, L.; Fleischauer, M. D.; Johnson, E. R.; White, M. A., Clusters in liquid fatty acids: structure and role in nucleation. *J. Phys. Chem. B* **2019,** *123* (32), 7043-7054.
10. Fan, P.; Wang, Y.; Shen, J.; Jiang, L.; Zhuang, W.; Han, Y.; Zhang, H., Self-assembly behaviors of C18 fatty acids in arginine aqueous solution affected by external conditions. *Colloids Surf. A Physicochem. Eng. Asp.* **2019,** *577*, 240-248.
11. Melis, M.; Mastinu, M.; Arca, M.; Crnjar, R.; Tomassini Barbarossa, I., Effect of chemical interaction between oleic acid and L-Arginine on oral perception, as a function of polymorphisms of CD36 and OBPIIa and genetic ability to taste 6-n-propylthiouracil. *PloS One* **2018,** *13* (3), e0194953.
12. Sebastiani, F.; Wolf, S. L. P.; Born, B.; Luong, T. Q.; Cölfen, H.; Gebauer, D.; Havenith, M., Water dynamics from THz spectroscopy reveal the locus of a liquid–liquid binodal limit in aqueous CaCO3 solutions. *Angew. Chem. Int. Ed.* **2017,** *56* (2), 490-495.
13. Soltani, A.; Gebauer, D.; Duschek, L.; Fischer, B. M.; Cölfen, H.; Koch, M., Crystallization caught in the act with terahertz spectroscopy: non-classical pathway for l-(+)-tartaric acid. *Chem. Eur. J.* **2017,** *23* (57), 14128-14132.
14. Choi, D.-H.; Son, H.; Jeong, J.-Y.; Park, G.-S., Correlation between salt-induced change in water structure and lipid structure of multi-lamellar vesicles observed by terahertz time-domain spectroscopy. *Chem. Phys. Lett.* **2016,** *659*, 164-168.
15. Yang, J.; Tang, C.; Wang, Y.; Chang, C.; Zhang, J.; Hu, J.; Lü, J., The terahertz dynamics interfaces to ion–lipid interaction confined in phospholipid reverse micelles. *ChemComm* **2019,** *55* (100), 15141-15144.
16. Jawor-Baczynska, A.; Moore, B. D.; Lee, H. S.; McCormick, A. V.; Sefcik, J., Population and size distribution of solute-rich mesospecies within mesostructured aqueous amino acid solutions. *Faraday Discuss.* **2013,** *167*, 425-40.
17. Chattopadhyay, S.; Erdemir, D.; Evans, J. M. B.; Ilavsky, J.; Amenitsch, H.; Segre, C. U.; Myerson, A. S., SAXS study of the nucleation of glycine crystals from a supersaturated solution. *Cryst. Growth Des.* **2005,** *5* (2), 523-527.
18. Baccile, N.; Cuvier, A.-S.; Prévost, S.; Stevens, C. V.; Delbeke, E.; Berton, J.; Soetaert, W.; Van Bogaert, I. N. A.; Roelants, S., Self-assembly mechanism of pH-responsive glycolipids: micelles, fibers, vesicles, and bilayers. *Langmuir* **2016,** *32* (42), 10881-10894.

19. Brotherton, E. E.; Hatton, F. L.; Cockram, A. A.; Derry, M. J.; Czajka, A.; Cornel, E. J.; Topham, P. D.; Mykhaylyk, O. O.; Armes, S. P., In situ small-angle X-ray scattering studies during reversible addition–fragmentation chain transfer aqueous emulsion polymerization. *J. Am. Chem. Soc.* **2019,** *141* (34), 13664-13675.
20. (a) Samanta, N.; Mahanta, D. D.; Choudhury, S.; Barman, A.; Mitra, R. K., Collective hydration dynamics in some amino acid solutions: A combined GHz-THz spectroscopic study. *J. Chem. Phys.* **2017,** *146* (12), 125101; (b) Heyden, M.; Sun, J.; Funkner, S.; Mathias, G.; Forbert, H.; Havenith, M.; Marx, D., Dissecting the THz spectrum of liquid water from first principles via correlations in time and space. *PNAS* **2010,** *107* (27), 12068-12073.
21. Jewariya, M.; Nagai, M.; Tanaka, K., Ladder climbing on the anharmonic intermolecular potential in an amino acid microcrystal via an intense monocycle terahertz pulse. *Phys. Rev. Lett.* **2010,** *105* (20), 203003.
22. Karaliūnas, M.; Nasser, K. E.; Urbanowicz, A.; Kašalynas, I.; Bražinskienė, D.; Asadauskas, S.; Valušis, G., Non-destructive inspection of food and technical oils by terahertz spectroscopy. *Sci. Rep.* **2018,** *8* (1), 18025.
23. Fan, S.; Ruggiero, M. T.; Song, Z.; Qian, Z.; Wallace, V. P., Correlation between saturated fatty acid chain-length and intermolecular forces determined with terahertz spectroscopy. *ChemComm* **2019,** *55* (25), 3670-3673.
24. Barrozo, A.; Xu, B.; Gunina, A. O.; Jacobs, M. I.; Wilson, K.; Kostko, O.; Ahmed, M.; Krylov, A. I., To be or not to be a molecular ion: the role of the solvent in photoionization of arginine. *J. Phys. Chem. Lett.* **2019,** *10* (8), 1860-1865.
25. Whitelam, S.; Jack, R. L., The Statistical Mechanics of Dynamic Pathways to Self-Assembly. *Annu. Rev. Phys. Chem.* **2015,** *66* (1), 143-163.
26. Brown, P.; Butts, C. P.; Eastoe, J., Stimuli-responsive surfactants. *Soft Matter* **2013,** *9* (8), 2365-2374.
27. Kanicky, J. R.; Shah, D. O., Effect of degree, type, and position of unsaturation on the pKa of long-chain fatty acids. *J. Colloid Interface Sci.* **2002,** *256* (1), 201-207.
28. (a) Salentinig, S.; Sagalowicz, L.; Glatter, O., Self-assembled structures and pKa value of oleic acid in systems of biological relevance. *Langmuir* **2010,** *26* (14), 11670-9; (b) Mele, S.; Söderman, O.; Ljusberg-Wahrén, H.; Thuresson, K.; Monduzzi, M.; Nylander, T., Phase behavior in the biologically important oleic acid/sodium oleate/water system. *Chem. Phys. Lipids* **2018,** *211*, 30-36.
29. Ilavsky, J., Nika: software for two-dimensional data reduction. *J. Appl. Crystallogr.* **2012,** *45* (2), 324-328.
30. Frisch, M. J.; Trucks, G. W.; Schlegel, H. B.; Scuseria, G. E.; Robb, M. A.; Cheeseman, J. R.; Scalmani, G.; Barone, V.; Mennucci, B.; Petersson, G. A.; Nakatsuji, H.; Caricato, M.; Li, X.; Hratchian, H. P.; Izmaylov, A. F.; Bloino, J.; Zheng, G.; Sonnenberg, J. L.; Hada, M.; Ehara, M.; Toyota, K.; Fukuda, R.; Hasegawa, J.; Ishida, M.; Nakajima, T.; Honda, Y.; Kitao, O.; Nakai, H.; Vreven, T.; J. A. Montgomery, J.; Peralta, J. E.; Ogliaro, F.; Bearpark, M.; Heyd, J. J.; Brothers, E.; Kudin, K. N.; Staroverov, V. N.; Keith, T.; Kobayashi, R.; Normand, J.; Raghavachari, K.; Rendell, A.; Burant, J. C.; Iyengar, S. S.; Tomasi, J.; Cossi, M.; Rega, N.; Millam, J. M.; Klene, M.; Knox, J. E.; Cross, J. B.; Bakken, V.; Adamo, C.; Jaramillo, J.; Gomperts, R.; Stratmann, R. E.; Yazyev, O.; Austin, A. J.; Cammi, R.; Pomelli, C.; Ochterski, J. W.; Martin, R. L.; Morokuma, K.; Zakrzewski, V. G.; Voth, G. A.; Salvador, P.; Dannenberg, J. J.; Dapprich, S.; Daniels, A. D.; Farkas, O.; Foresman, J. B.; Ortiz, J. V.; Cioslowski, J.; Fox, D. J., *Gaussian 09, Revision C.01, Gaussian, Inc., Wallingford CT, 2010.*
31. Tomasi, J.; Mennucci, B.; Cammi, R., Quantum mechanical continuum solvation models. *Chem. Rev.* **2005,** *105*, 2999-3093.
32. Alecu, I. M.; Zheng, J.; Zhao, Y.; Truhlar, D. G., Computational Thermochemistry: Scale factor databases and scale factors for vibrational frequencies obtained from electronic model chemistries. *J. Chem. Theory Comput.* **2010,** *6* (9), 2872-2887.
33. Parrott, E. P. J.; Zeitler, J. A., Terahertz time-domain and low-frequency raman spectroscopy of organic materials. *Appl. Spectrosc.* **2015,** *69* (1), 1-25.

Figures

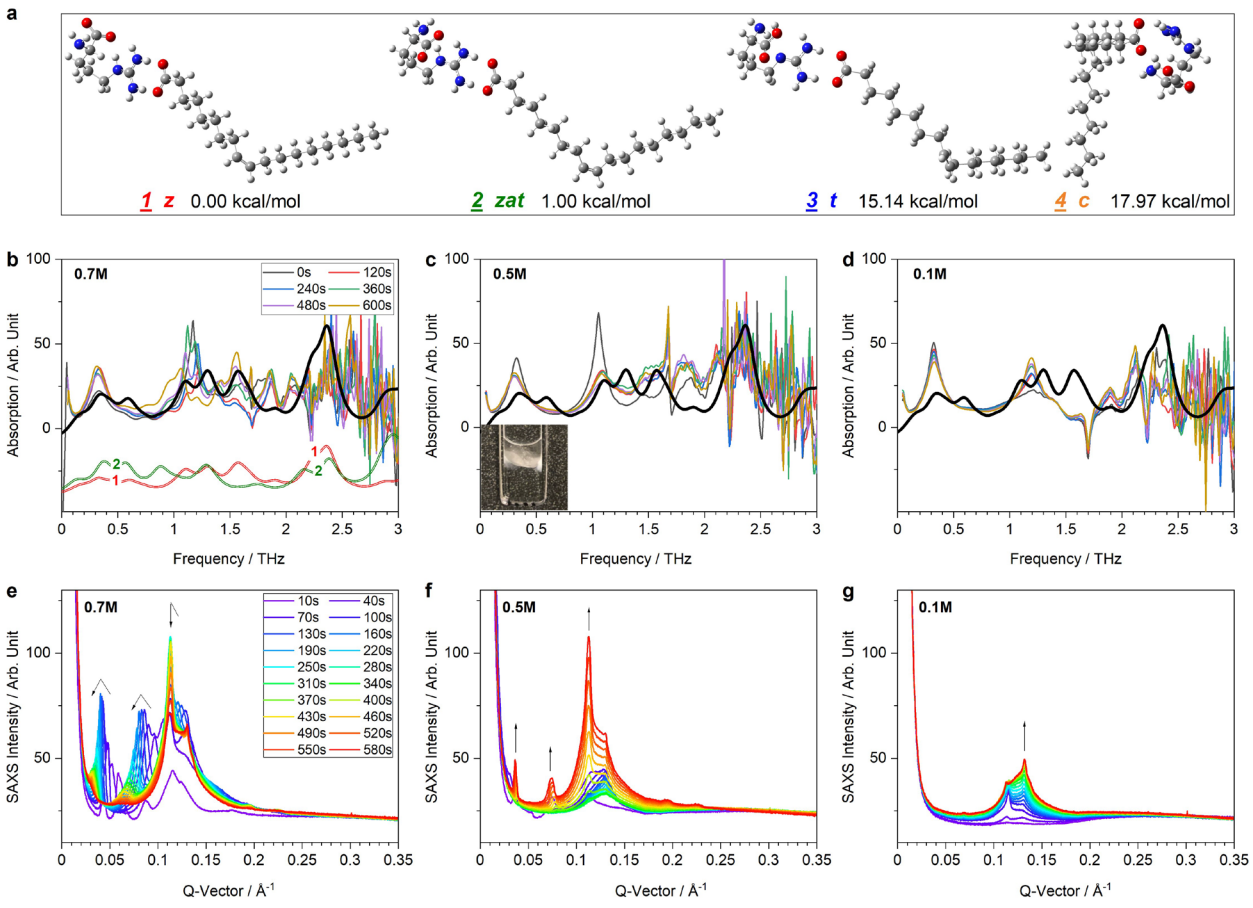

Figure 1. (a) The most stable Arg-Ole conformers built from 4 arginine tautomers (*z*-, *zat*-, *t*-, and *c*-), optimized at the ωB97XD/PCM/ 6-31+G(d,p) level of theory; **(b)** – **(d)** THz spectra collected for the first 10 minutes at the Arg-Ole interface of 0.7, 0.5, and 0.1M, pH = 11 arginine solution. The red and green curves in **(b)** are the calculated THz spectra of the *z*- and *zat*- conformers in **(a)**, and the black thick curve is the linear combination of the 2 calculated spectra weighed by their populations at 298K. The inset in **(c)** shows the formation of white aggregates upon addition of pure oleic acid to 0.5M arginine solution; and **(e)** – **(g)** SAXS spectra collected during the first 10 minutes at the Arg-Ole interface of 0.7, 0.5, and 0.1M, pH = 11 arginine solution. The black arrows in each frame indicate the position change of each peak.

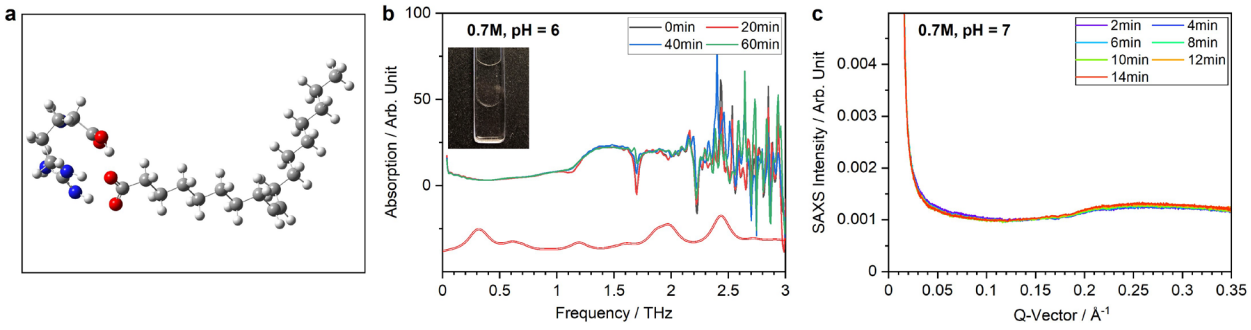

Figure 2. (a) The lowest-free-energy conformer of $ArgH^+$-Ole optimized at ωB97XD/PCM/6-31+G(d,p) level of theory; **(b)** 0-, 20-, 40- and 60-min THz measurement at the Arg-Ole interface of 0.7M, pH = 6 arginine solution. The red curve is the calculated THz spectra derived from the structure in **(a)**. The inset shows two clear immiscible liquid phases without reaction; and **(c)** SAXS spectra of the first 14 minutes at the Arg-Ole interface of 0.7M, pH = 7 arginine solution.

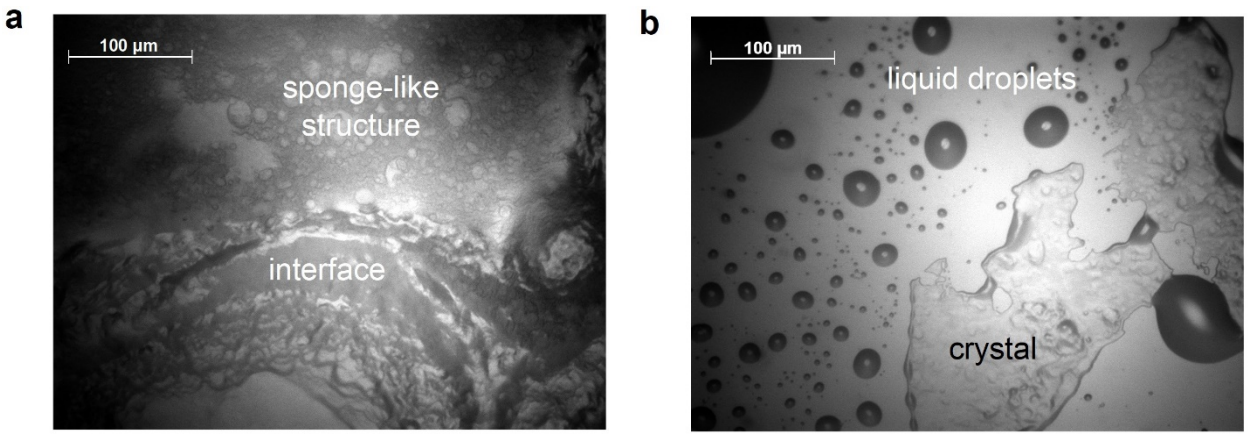

Figure 3. (a) The microscopic image showing morphology and structure of the "sponge-like" aggregates formed via self-assembly of Arg-Ole system; and **(b)** a thin-layer cross-section view of the aggregate slice. The dark-colored dots represent liquid droplets from the two liquid phases.

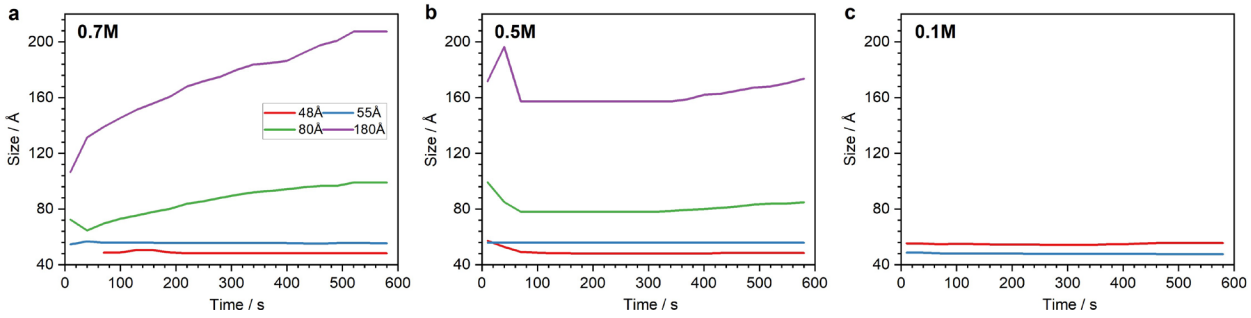

Figure 4. The kinetic analysis of first 10 minutes of the SAXS peaks at the Arg-Ole interface of **(a)** 0.7, **(b)** 0.5 and **(c)** 0.1M, pH = 11.